THERMO-MECHANICAL PROCESSING IN A SYNCHROTRON BEAM - FROM SIMPLE METALS TO MULTIPHASE ALLOYS AND INTERMETALLICS

Klaus-Dieter Liss

Australian Nuclear Science and Technology Organisation
New Illawarra Road, Lucas Heights, NSW-2234, Australia - liss@kdliss.de, kdl@ansto.gov.au

Introduction

The mechanical properties of a metallic product depend strongly on both phase composition and microstructure of a polycrystalline product and large development efforts for the design of novel materials deal with these issues. Besides the physical parameters, the artwork is to perform the right thermo-mechanical processing, which for highly designed materials can be very sophisticated. Therefore, thermo-mechanical simulators are widely used in industry and laboratories (Figure 1). They not only allow to obtain experimental results for fundamental knowledge, understanding and design of a new bulk material but also the study of very particular and applied cases.

Conventional methods of materials characterization are ex-situ and conducted following time-consuming post-mortem preparation. For example, a metal is processed under realistic or model conditions at high temperature, with a defined time and stress profile and then quenched to freeze the structure from that particular point in parameter space. To access its bulk properties, this specimen is then cut, polished and examined by microscopy or conventional X-ray diffraction in near-surface region. In order to obtain the material's behavior along several time steps of the thermo-mechanical process, a second, third and many further specimens are prepared from slightly different temperature or stress states and subsequently analyzed. These traditional techniques are time consuming and it is usually not clear whether the microstructure developed during the processing is still the same after quenching, particularly when subsequent phase transformations are involved.

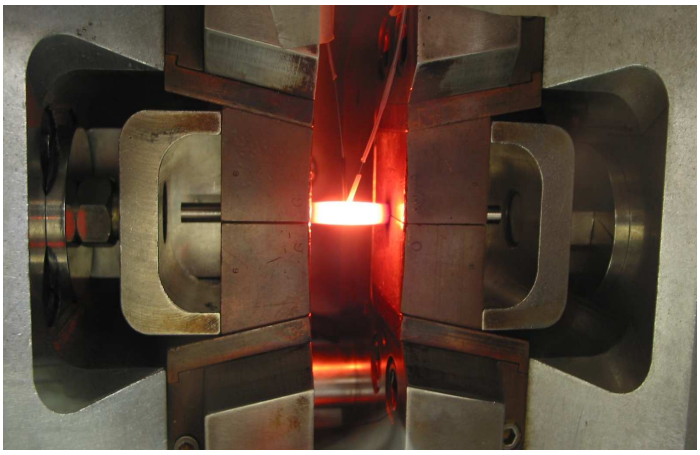

Figure 1: *Glowing specimen during physical thermo-mechanical testing in a Gleeble® simulator. Photo and setup by Kevin Thorogood [0].*

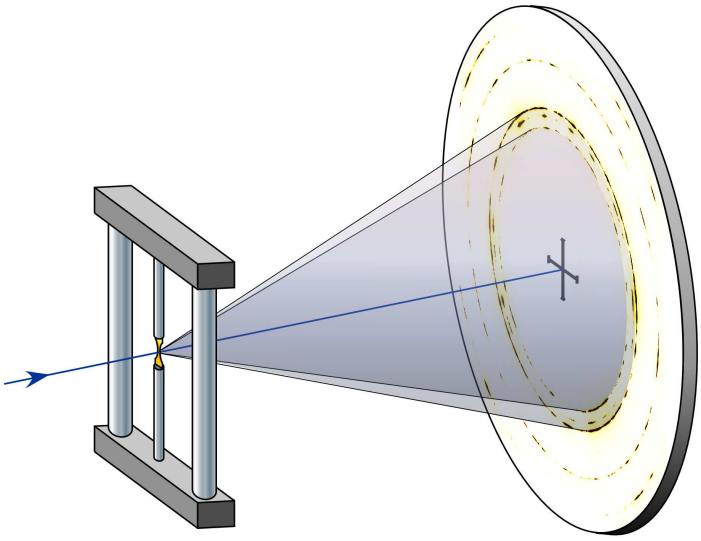

Figure 2: *Experimental setup. A fine synchrotron beam enters the scenario from the left, scatters at the sample, located in the load frame and is detected to the right.*

Put a Gleeble® in the beam

The intensity of high brilliant synchrotron beams is adequate to record X-ray diffraction movies in real time, in-situ, during heating ramps or under physical thermo-mechanical simulation.

High energy X-rays bear the advantage of deep penetration into materials and therefore can be employed for the investigation of the bulk and in embedded environments [1]. With an energy of 10 times higher than conventional X-rays, photo absorption becomes about 1000 times weaker, allowing, for example, to study many centimeters thick steel. In addition, when such radiation is produced with undulators at high energy synchrotrons, beams can be very small with dimensions between 1 µm and 100 µm, which is comparable to the grain size of the microstructure in typical metals, bearing the opportunity to gather single grain information.

Traditional X-ray powder diffraction is based on an average of reflections from many tens of thousands of crystallites leading to an intensity distribution as a function of scattering angle. Peaks are observed at angles, where Bragg's law is fulfilled, i.e. where the X-ray wavelength matches the path length between neighboring lattice planes. The so-obtained intensity profiles can be used in search-match software to determine the phase composition in multiphase or composite materials. Sophisticated fitting by the Rietveld method allows to exploit those patterns for structural determination and

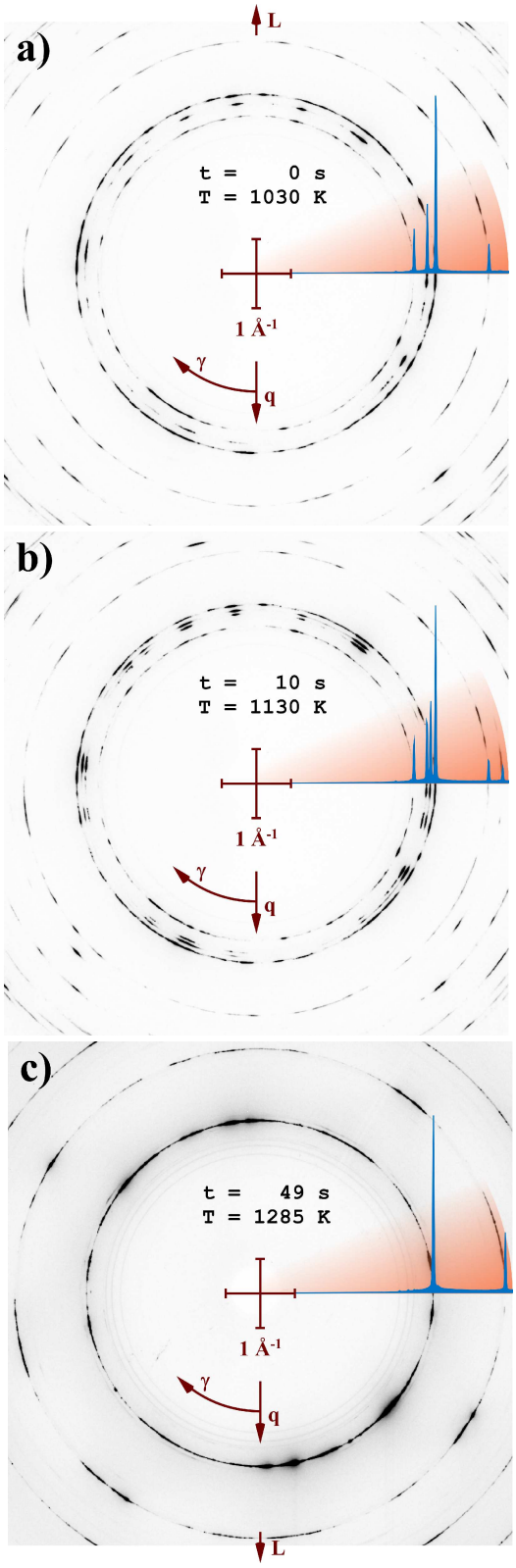

Figure 3: *Three representative 2D diffraction patterns from Zircaloy-4 undergoing a heating ramp upon plastic deformation, a) in the α-phase, b) in the α+β-phase and c) in the β-phase field.*

many other parameters of a distorted crystal model.

In the recent years, electronic 2-dimensional (2D) detectors became available which have been mostly used to collect more intensity over larger solid angle. Often, a sample with a large grain size, or with only a small number of grains in the illuminated volume, shows so-called spottiness along the Debye-Scherrer rings in the 2D diffraction patterns. This is, when distinguished crystallites are particularly well oriented for reflection. The powder average is not given any more and the intensity profile depends not only on the structure of the material, but also on the orientation of the crystallites.

In contrast, the present research particular takes advantage of the spottiness to gather information about the grain size, orientation distribution and grain perfection. It can reveal grain refinement and growth, grain correlations, orientation correlations, texture, subgrain formation, recovery and recrystallization – in-situ, in real time and from the bulk of the material.

Experimental setup

Experiments were performed at both beamline 1-ID at the Advanced Photon Source (APS), USA, and beamline ID15B at the European Synchrotron Radiation Facility (ESRF), France. A fine, collimated beam of approximately Ø 50 µm, X-ray energy E = 90 keV, wavelength λ = 0.14 Å and wavenumber k = 46 Å^{-1} impinges onto the polycrystalline specimen and scatters into Debye-Scherrer rings, recorded in 1 m – 2 m distance by a fast, 2D detector, see Figure 2. Due to the small wavelength, diffraction angles are within 0 ~ 15° allowing to probe the sample in transmission geometry. Only small apertures into potentially bulky sample environments are needed, leaving considerable space for complex ancillaries. For the present investigations, we used different load frames for room temperature or equipped with radiative or electric resistance heating gear. In principle, any such apparatus can be inserted into the beamlines.

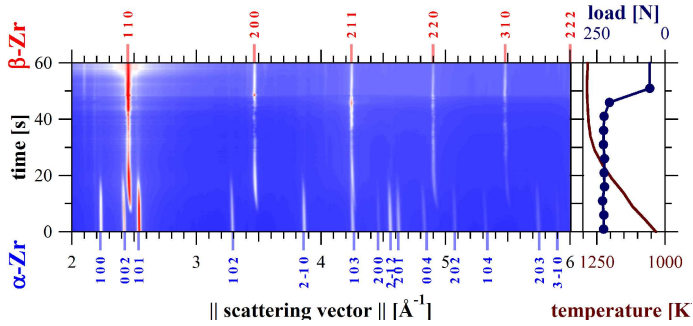

Figure 4: *Color coded diffraction patterns (left) as a function of time while the specimen is ramped in temperature and under mechanical load (right).*

Data presentation

Representative, 2D diffraction images from zirconium alloy are shown in Figure 3 at three different times t and temperatures T during a physical thermo-mechanical simulation test. The cross denotes the center of the Debye-Scherrer rings, origin of reciprocal space. The radial direction q corresponds to diffraction angles 2θ, calibrated to scattering vector units $q = 4\pi/\lambda \sin(\theta)$, which are linear and independent of the radiation used. Integration along the azimuthal angle γ leads to conventional, 1D powder diffraction patterns I(q,t) and are displayed as a color-intensity plot in Figure 4. Peak positions, as indexed here for α-Zr and β-Zr, and intensities can be used for lattice

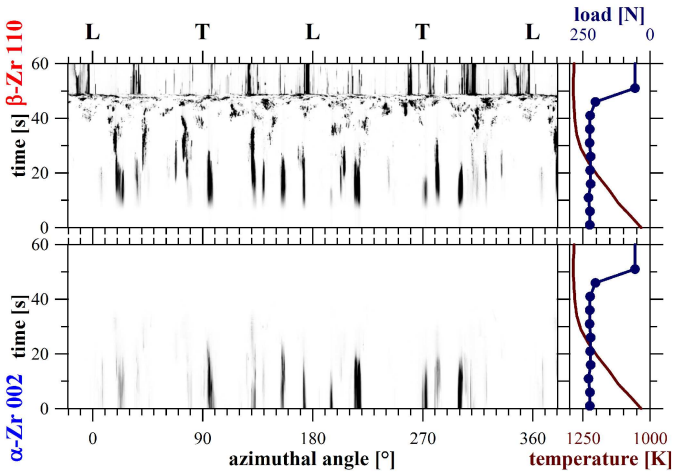

Figure 5: *AT-plots derived from the Debye-Scherrer rings in Figure 3 and as indexed in Figure 4.* ***L*** *and* ***T*** *denote the longitudinal and transverse load direction, respectively [4].*

parameter and phase evaluation [2, 3].

The 2D diffraction images from Figure 3 contain complementary information in the azimuthal-angle direction. The morphology along the Debye-Scherrer rings varies as a function of time, when phase transformations or plastic deformation take place. The salient feature of the present article is to display and extract useful information about the evolution of the microstructure of the specimen. In principle, a low number of reflection spots corresponds to a small number of reflecting grains and thus, large grain size. The angular width of a spot represents the mosaic distribution, which is due to distortion by a subgrain structure such as dislocations, dislocation cells or any kind of small angle grain boundaries.

In order to display the spottiness as a function of time, a selected Debye Scherrer ring is cut and straightened into a line of Figure 5. In this way, the intensity of the α-Zr 002 reflection from Figure 3a, the second inner ring as indexed in Figure 4, is reproduced in a horizontal line at t = 0 s of Figure 5 while the third inner ring from Figure 3b goes into the β-Zr 110 plot of Figure 5 at time t = 10 s. We call these diagrams azimuthal-angle / time plots (AT-plots) and denote as timelines the appearing intensities streaking in time.

Hot deformation of zirconium alloy

Zirconium alloys such as Zircaloy and Zr-2.5Nb bear an important group of materials in the nuclear reactor industry. The present study focuses on Zircaloy-4 of nominal composition Zr $_{1.5}$Sn $_{0.2}$Fe $_{0.1}$Cr $_{0.1}$O (wt %) and an estimated grain size of a few 100 µm. Between 1083 K and 1253 K, it transforms from the *hcp* α-Zr to the *bcc* β-Zr structure. The specimen of initially 6 mm^2 cross section was constantly loaded under tension with 225 N and the temperature was ramped from 688 K to 1283 K in 60 s while diffraction patterns were taken with a frame rate of 5 Hz [4].

The experimental data is presented in Figures 3–5. The phase transformation is well seen in Figure 4 by the disappearance of the α-Zr and the appearance of the β-Zr lines. Figure 3b shows a snapshot in the α+β-Zr two-phase field. As a direct result, the intensity spots on the appearing β-Zr 110 ring are well aligned with the spots on the ceasing α-Zr 002 and, to a lesser extend, α-Zr 101 rings, revealing the Burgers and Potter orientation relationships of the crystal lattices upon transformation.

The AT-plot of α-Zr 002 in Figure 5 consists of vertical timelines, revealing that no new grain orientations of this phase appear. All timelines disappear upon the phase transformation, but some cease earlier, indicating slight grain growth. The timelines of β-Zr 110 appear exactly at the positions of α-Zr 002, underlining above mentioned orientation relationships. After further grain growth, the β-Zr 110 timelines become interrupted, dotty, and split into laterally finer features (around t ~ 30 s). This dottiness stems from slight fluctuations in angle and time, and represent the process of dynamic recovery. By gentle plastic flow, dislocations are continuously introduced into the grains, driving to increase their mosaic spread. Local recovery, however, counteracts and creates zones of perfect crystals, subgrains, which may be separated through a small-angle grain boundary from each other. As the deformation continues, this process repeats itself over and over again, leading to those fluctuations. On progress, necking occurs and the temperature still raises, leading to faster and faster plastic deformation. At around t ~ 40 s, larger jumps in azimuthal angle occur. New timelines and thus new grain orientations appear in angular regions where nothing has been observed before, which is dynamic recrystallization. The process is similar to dynamic recovery, but happens on a grain rather than a subgrain scale, typically leading to larger jumps in orientation space. On top of this, strong dottiness can be observed within the new born timelines revealing dynamic recovery in the new grains until they disappear again.

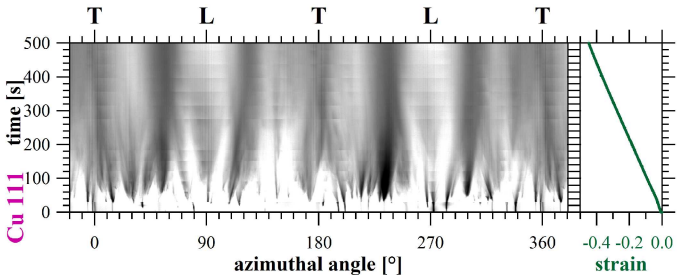

Figure 6: *AT-plot of copper undergoing compression at room temperature (left) with strain evolution (right) [5].*

Compression of copper at room temperature

A specimen of annealed copper with grain size of ~300 µm has been tested under compression to ε = -48% [5]. The AT-plot for the Cu 111 reflection is given in Figure 6. The features in the timelines of this room temperature test differ strongly from the high temperature test on Zircaloy. The few spots at the beginning evolve into continuously broadening timelines. Furthermore, many timelines are inclined, which reveals grain rotation around the beam axis. Finally, the timelines of the individual grains merge, leading to a modulated orientation distribution, the final texture of the material.

Grain rotation is well known to occur on plastic

deformation under crystallographic slip. The grains rotate towards their textural preferred orientation and, in this case, matches well the predicted fiber texture. The broadening of the timelines occurs when grains evolve into strongly distorted subgrains through a continuous introduction of dislocations. Eventually, subgrain structures behave like individual grains and tend to rotate under further plastic deformation. This process can lead to very large orientation distributions. In contrast to the hot deformation, no grain recovery process exists.

Hot deformation in two-phase titanium aluminium

Titanium aluminium intermetallics are being developed as light weight, high temperature structural materials for the aerospace and transportation industry. A particular novel development is so-called TNM™ alloy of nominal composition Ti-43.5Al-4Nb-1Mo-0.1B (at.%) which exposes all three phases, near-*fcc* γ-, *hcp* α- and *bcc* β-phase. Details may slightly vary according to atomic order and disorder [6].

Figure 7 displays the AT-plots for the overlapping γ-111 / α-002 and the β-110 reflections upon heating to the processing temperature at 1573 K and subsequent compression to -63%. While the γ-111 timelines disappear at the phase transformation at T_α = 1555 K, all timelines are merely constant until plastic deformation sets on. Again, α- and β-phased display the well known orientation relationships, proving that they previously were formed from a common mother grain through a phase transformation. Eye-popping differences exist, however, in the individual deformation behavior of the two phases. The β-phase quickly develops mosaic spread, i.e. subgrains, which quickly recover dynamically, resulting in a fluctuating, but isotropic orientation distribution. The α-phase, however, shows many features as seen upon the room temperature deformation of Cu, which are grain rotation, to some extend continuous mosaic broadening and the formation of a tilted basal texture. These fingerprints for predominant slip deformation are superimposed by slow dynamic recovery and even slower dynamic recrystallization, which can be recognized by elongated subgrain (dotted) timelines and accumulations of timelines appearing and disappearing with larger angular offset.

Conclusion

Grain sensitive, time resolved, in-situ diffraction experiments together with novel approaches in data analysis have been developed to investigate polycrystalline materials undergoing structural and microstructural changes, such as under thermo-mechanical processing. The method gains insight into grain size effects, mosaic spread and subgrain evolution, grain rotation, the formation of texture, elastic lattice strain, phase transformations. It allows to distinguish the deformation mechanisms of slip, twinning [7], dynamic recovery and dynamic recrystallization. It not only delivers the responses in real time, but also allows to assess the behavior of coexisting phases simultaneously.

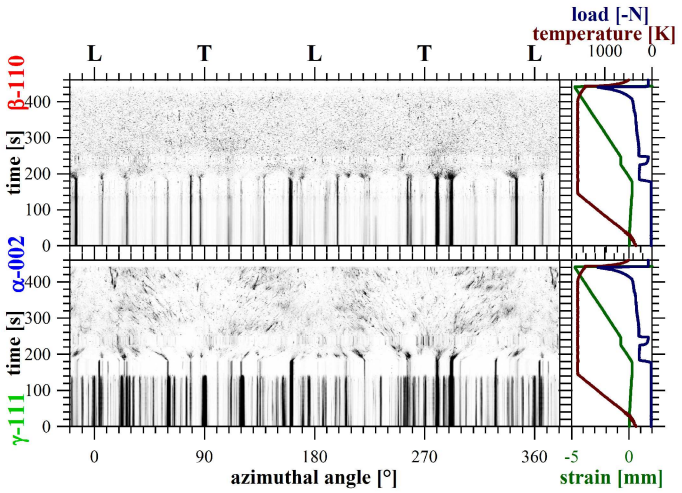

Figure 7: *AT-plots of α-β-γ-TiAl based intermetallics undergoing deformation in the α+β-phase field [6].*

Applications are not limited to the field of metallurgy and can be expanded to all kind of polycrystalline materials in its widest sense.

The time is ripe that industries take competitive advantage and install large scale thermo-mechanical simulation on existing and new synchrotron facilities in order to perform such investigations routinely for the design of new materials.

Acknowledgements

The author likes to thank his collaborators K. Yan, R. Dippenaar, H. Clemens, H. Li, R.P. Harrison, U. Garbe, M. Reid, T. Schambron, D.G. Carr, J. Daniels, J. D. Almer, T. Buslaps, M. Peel for providing the materials, experimental support and constructive discussions.

Access to the APS was supported by the Australian Synchrotron Research Program (ASRP), which was funded by the Commonwealth of Australia under the National Collaborative Research Infrastructure Strategy. Use of the APS was supported by the U.S. Department of Energy under contract DE-AC02-06CH11357.

We acknowledge travel funding to the ESRF provided by the International Synchrotron Access Program (ISAP) managed by the Australian Synchrotron. The ISAP is funded by a National Collaborative Research Infrastructure Strategy grant provided by the Federal Government of Australia.

References

[0] Kevin Thorogood: `*The Effect of Welding Thermal Cycles on the Microstructure and Texture of Zircaloy-4'*, Bachelor of Engineering Thesis, University of Wollongong, (2007).
[1] K.-D. Liss, A. Bartels, A. Schreyer, H. Clemens: Textures and Microstructures, 35 (3/4) (2003) 219-252
[2] L. A. Yeoh, K.-D. Liss, A. Bartels, H. F. Chladil, M. Avdeev, H. Clemens, R. Gerling, T. Buslaps: Scripta Materialia 57 (2007) 1145-1148.
[3] K. Yan, D.G. Carr, S. Kabra, M. Reid, A. Studer, R.P. Harrison, R. Dippenaar, K.-D. Liss: World Journal of Engineering, (current issue, 2010)
[4] K.-D. Liss, U. Garbe, H. Li, T. Schambron, J. D. Almer, K. Yan: Advanced Engineering Materials, 11/8 (2009) 637-640
[5] K. Yan, K.-D. Liss, U. Garbe, J. Daniels, O. Kirstein, H. Li, R. Dippenaar: Advanced Engineering Materials, 11/10 (2009) 771-773
[6] K.-D. Liss, T. Schmoelzer, K. Yan, M. Reid, M. Peel, R. Dippenaar, H. Clemens: Journal of Applied Physics, 106/11, (2009) 113526
[7] K. Yan, D.G. Carr, M.D. Callaghan, K-D. Liss, H. Li: Scripta Materialia 62 (2010) 246-249